Neurobiology of Aging 74 (2019) 213–224

Contents lists available at ScienceDirect

Neurobiology of Aging

journal homepage: www.elsevier.com/locate/neuaging

# Neuroendocrine aging precedes perimenopause and is regulated by DNA methylation

Eliza R. Bacon [a], Aarti Mishra [b], Yiwei Wang [b], Maunil K. Desai [b], Fei Yin [c], Roberta Diaz Brinton [a,b,c,*]

[a] Neuroscience Graduate Program, University of Southern California, Los Angeles, CA, USA
[b] Clinical Pharmacy and Pharmaceutical Economics and Policy, School of Pharmacy, University of Southern California, Los Angeles, CA, USA
[c] Center for Innovation in Brain Science, College of Medicine Tucson, University of Arizona, Tucson, AZ, USA

ARTICLE INFO

*Article history:*
Received 15 January 2018
Received in revised form 21 September 2018
Accepted 21 September 2018
Available online 5 October 2018

*Keywords:*
Menopause
Perimenopause
Aging
Epigenetics
DNA methylation
Hypothalamus

ABSTRACT

Perimenopause marks initiation of female reproductive senescence. Age of onset is only 47% heritable suggesting that additional factors other than inheritance regulate this endocrine aging transition. To elucidate these factors, we characterized transcriptional and epigenomic changes across endocrine aging using a rat model that recapitulates characteristics of the human perimenopause. RNA-seq analysis revealed that hypothalamic aging precedes onset of perimenopause. In the hypothalamus, global DNA methylation declined with both age and reproductive senescence. Genome-wide epigentic analysis revealed changes in DNA methylation in genes required for hormone signaling, glutamate signaling, and melatonin and circadian pathways. Specific epignetic changes in these signaling pathways provide insight into the origin of perimenopause-associated neurological symptoms such as insomnia. Treatment with 5-aza-2′-deoxycytidine, a DNA-methyltransferase-1 inhibitor, accelerated transition to reproductive senescence/ whereas supplementation with methionine, a S-adenosylmethionine precursor, delayed onset of perimenopause and endocrine aging. Collectively, these data provide evidence for a critical period of female neuroendocrine aging in brain that precedes ovarian failure and that DNA methylation regulates the transition duration of perimenopause to menopause.



## 1. Introduction

Perimenopause marks the initiation of the transition into female reproductive senescence and is characterized by the exhaustion of oocytes, amenorrhea, and the loss of cyclic estrogen production (Brinton et al., 2015). In women, the perimenopausal transition can span several years and timing of onset, duration, and completion has been linked to differential neurocognitive health outcomes (Geerlings, 2001; Rocca, 2011; Brinton et al., 2015). Age of onset is only 47% heritable (Byars et al., 2010), and variability is present in monozygotic twins (Snieder et al., 1998) and inbred rat strains (Finch, 2014), suggesting that epigenetics and environmental factors play important roles in reproductive aging. Indeed, recent studies in both humans and rats have demonstrated an association between reproductive senescence and changes in the epigenome (Levine et al., 2016). In humans, postmenopausal women exhibit accelerated patterns of epigenetic aging compared with premenopausal women of the same biological age (Levine et al., 2016). However, the cause-effect relationship between epigenetics and reproductive senescence remains unclear. Untangling this relationship will prove challenging as differences in epigenetic patterns seen across the perimenopause transition most likely consist of environmental and age-related changes that initiate onset of reproductive senescence, as well as changes that occur as a direct result of fluctuating sex hormones.

Establishment, maintenance, and reorganization of the epigenome rely on the availability of methyl-donor molecules that are produced from one-carbon metabolism. The one-carbon cycle uses co-factors such as folate, choline, and various other B vitamins (B6, B12, riboflavin), to recycle homocysteine to produce S-adenosylmethionine (SAM), the universal methyl-donor that provides methyl-groups used for DNA, histone, and other protein methylation. Breakdown of the one-carbon cycle results in decreased production of SAM and an accumulation of the intermediate molecule, homocysteine (Herrmann and Obeid, 2011; Tomizawa et al., 2015). Failure to produce sufficient levels of SAM can lead to global decline of DNA and histone methylation, resulting in

* Corresponding author at: Center for Innovation in Brain Science http://cibs.uahs.arizona.edu/, College of Medicine, University of Arizona, 1501 North Campbell Avenue, P.O. Box 245126, Tucson, AZ 85724-5126, USA. Tel.: +1 520 626 4681; fax: +(520)626-4884.
*E-mail address:* rbrinton@email.arizona.edu (R.D. Brinton).

0197-4580/$ – see front matter © 2018 Elsevier Inc. All rights reserved.
https://doi.org/10.1016/j.neurobiolaging.2018.09.029

dysregulation of the epigenome. One-carbon metabolism varies among individuals and has been shown to fluctuate with age and menopausal status (Zeisel, 2009). Furthermore, elevated plasma homocysteine has been observed in both postmenopausal women (Hak et al., 2000) and patients with Alzheimer's disease (Nazef et al., 2014; Shen and Ji, 2015; Zeisel 2009), linking reproductive senescence to increased risk for neurocognitive disease later in life, possibly through epigenetic mechanisms.

The sequence of events leading up to reproductive senescence is complicated. Reproductive senescence is not solely initiated by ovarian depletion of oocytes but, rather, is a function of both ovarian failure and hypothalamic aging. The hypothalamic-pituitary-gonadal (HPG) axis, which is activated during puberty, is a negative-feedback system in which pulsatile gonadotropin-releasing hormone (GnRH) produced in the hypothalamus stimulates luteinizing hormone (LH) and follicle-stimulating hormone (FSH) production and secretion by the pituitary. LH and FSH then stimulate estrogen and production in the ovaries. Systemic estrogen then feeds back onto the pituitary and hypothalamus to modulate GnRH, LH, and FSH production and secretion (Davis et al., 2015). Pituitary response to GnRH and ovarian response to LH and FSH simultaneously decline with age resulting in the diminished sex steroid production characteristic of reproductive senescence and a loss of negative feedback resulting in increased GnRH, LH, and FSH production (Bottner et al., 2007; Davis et al., 2015).

Preliminary evidence suggests that impaired one-carbon metabolism precedes decline in ovarian function and may be partially responsible for initiating reproductive senescence. Dietary supplements of folate (vitamin B9) have been shown to increase luteal progesterone levels in premenopausal women and decrease risk for sporadic anovulatory cycles (Gaskins et al., 2012). We hypothesize that one-carbon metabolism has the ability to regulate the estrus cycle and modulate initiation of reproductive senescence through loss of methyl-donor production needed to properly maintain the epigenome.

## 2. Methods

### 2.1. Animals

Animal studies were performed following National Institutes of Health guidelines on use of laboratory animals; protocols were approved by the University of Southern California Institutional Animal Care and Use Committee. A total of 201 young or middle-aged female Sprague-Dawley rats were obtained from Envigo Laboratories. Daily assessment of endocrine cycling of female rats was conducted from 5 to 12 months of age using rats that had given birth to at least one litter. Ovarian-function/cycle status was evaluated daily by the cytology of uterine cells obtained from lavage at 11 am. The smear was morphologically characterized based on the four stages of the cycle: estrus (E), metestrus (M), diestrus (D), and proestrus (P). The regular 4- to 5-day estrus cycle is defined as the period between successive estrus smears (E, M, D, P, E, M, D, P, E). In addition to regular cycling animals, selected groups included middle-aged rodents at defined stages of "peri-menopause" (Fig. 1B). The irregular group was defined as 2 contiguous cycles of >5 days characterized by prolonged diestrus stages. The acyclic (constant estrus) group was defined as persistent vaginal cornification lasting >8 days. Rats at designated age (6 months or 9–10 months) and cycling status were euthanized at estrus or constant estrus. Five sets of animals were used in this study. The first set (85 rats in total) included all 4 experimental groups (Reg-6m, Reg-9 to 10m, Irreg-9 to 10m, and Acyc-9 to 10m). Of this set, N = 5–6 per group were used for DNA methylation analysis. A second set of rats, containing all four groups, (40 rats in total) was used for RNA-seq analysis. A third set of rats (30 rats in total) was used to assess timing of peri-menopause onset, duration, and completion. Cycling status of these animals was monitored from 9 months' regular cycling until they reached constant estrus. The fourth set of rats, containing only the Reg-6m group, (20 rats in total) was used for 5-aza-2'-deoxycitidine treatment. A fifth set of rats, containing only the Reg-6m group, (26 rats in total) was used for methionine treatment. Rats that did not meet the endocrine criteria for each group were excluded from analyses for this study.

### 2.2. 5-Aza-2'-deoxycitidine treatment

5-Aza-2'-deoxycitidine-saline solution of 0.1 mg/mL was prepared fresh for each use and stored on ice (Sigma-Aldrich). Animals (N = 6 per group) were subcutaneously injected with 0.25 mg/kg drug, or an equivalent volume of saline, three times weekly (Monday, Wednesday, Friday) beginning at 6 months of age and until 9 months when cycle status was assessed.

### 2.3. Methionine treatment

Methionine-H2O stock solution of 50 mg/mL will be prepared and stored (Sigma-Aldrich). Regularly cycling animals were subcutaneously injected with 50 mg/kg, 100 mg/kg, and 200 mg/kg of methionine, or an equivalent volume of H2O, three times weekly (Monday, Wednesday, Friday) beginning at 6 months of age and until 10 months when cycle status was assessed. All three methionine treatment groups were combined for analysis (n = 7) against the vehicle group (n = 4).

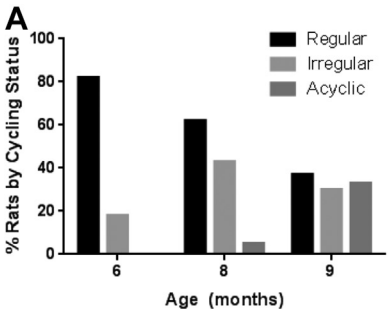


B

| Cycling Status | Age (months) | Body Weight (g) | Uterine Weight (g) |
|---|---|---|---|
| Regular | 6 | 272±4* | 0.57±0.03 |
| Regular | 9 | 295±2 | 0.64±0.03 |
| Irregular | 9 | 294±2 | 0.61±0.03 |
| Acyclic | 9 | 285±4 | 0.59±0.03 |

**Fig. 1.** Phenotypic characterization of endocrine aging of female rats during endocrine aging. (A) Transition of cycling stages with age: percentage of aging rats by cycling status from a cohort of 85 rats. (B) Body and uterine weight of animals with different age and cycling status. Data were presented as average ± SEM, $^{*}p \leq 0.0001$, n = 9–20.

### 2.4. Tissue collection

For the first two sets of animals, rats were euthanized and the brains rapidly dissected on ice. Cerebellum, brainstem, and hypothalamus were removed from each brain, and the two hemispheres were separated. The cortical hemisphere was fully peeled laterally, and the hippocampus was then separated. Cerebellum, midbrain, brainstem, hypothalamus, and both cortexes and hippocampi were harvested and frozen at −80°C. Ovaries and uterus were harvested and frozen at −80°C.

### 2.5. Nucleic acid extraction

Total RNA was extracted from tissue homogenized in TRIzol and purified using the PureLink RNA Mini Kit (Thermo Fisher Scientific). RNA was DNase treated on column during purification (Thermo Fisher Scientific). DNA was extracted from tissue homogenized in lysis buffer [10 mM Tris-HCl (pH 8.0), 1 mM EDTA, 0.1% SDS], RNase treated (Zymo Research Corp., Irvine, CA), purified using phenol/chloroform/isoamyl alcohol, and then precipitated in isopropanol.

### 2.6. RNA-seq

Total RNA-seq libraries were constructed from RNA extracted from the hypothalamus of female rats. Samples were run on the Illumina HiSeq 2500 using 50 bp Pair ended reads to obtain a total read depth of roughly 50 million read pairs per sample. Raw data files in the FASTQ format underwent QA/QC and trimming procedure in the cloud-based Partek Flow environment (http://www.partek.com/). The paired end reads for each sample were then aligned using TopHat to the rat reference genome rn6 (Ensembl 80). Transcript assembly and quantification of aligned reads were carried out using Cufflinks. The Cufflinks output consisted of a list of differentially expressed genes for each comparison.

### 2.7. RNA-seq bioinformatic analysis by Ingenuity Pathway Analysis

Expression data for genes with the $p$-value $< 0.05$ were analyzed by Ingenuity Pathway Analysis (IPA) core analysis composed of a network analysis and an upstream regulator analysis. We used these relaxed criteria to maximize the coverage of the gene array results in the bioinformatic analyses. The network analysis identified biological connectivity among molecules in the data set that were upregulated or downregulated in a comparison (focus molecules that serve as "seeds" for generating networks) and their interactions with other molecules present in the Ingenuity Knowledge Base. Focus molecules were combined into networks that maximized their specific connectivity. Additional molecules from the Ingenuity Knowledge Base (interacting molecules) were used to specifically connect two or more smaller networks to merge them into a larger one. A network was composed of direct and indirect interactions among focus molecules and interacting molecules, with a maximum of 70 molecules per network. Generated networks were ranked by the network score according to their degree of relevance to the network eligible molecules from the data set. The network score was calculated with Fisher's exact test, taking into account the number of network eligible molecules in the network and the size of the network, as well as the total number of network eligible molecules analyzed and the total number of molecules in the Ingenuity Knowledge Base that were included in the network. Higher network scores are associated with lower probability of finding the observed number of network eligible molecules in a given network by chance.

IPA Upstream Regulator Analysis is a tool that predicts upstream regulators of observed gene expression changes based on the published literature and compiled in the Ingenuity Knowledge Base. The analysis identifies the known targets of each transcription regulator that is present in the data set and compares the direction of change to what is expected based on published literature to predict transcriptional regulators. If the observed direction of change is consistent with a particular activation state of the transcriptional regulator ("activated" or "inhibited"), then a prediction is made for that activation state (z-score). For each potential regulator two statistical measures, an overlap $p$-value, and an activation z-score are computed. The overlap $p$-value identifies likely upstream regulators based on significant overlap between data set genes and known targets regulated by a regulator. The activation z-score is used to infer likely activation states of upstream regulators based on comparison with a model that assigns random regulation direction. The upstream regulator list is generated using computational predictions and is not based on experimental evidence in the rat model used in this study. Although in practice, z-scores greater than 2 or smaller than −2 can be considered significant, our particular interest was in identifying upstream regulators potentially controlling transcription across the endocrine transition states. Thus, all molecules with significant $p$-values regardless of z-score were further evaluated.

### 2.8. Global DNA methylation analysis

Genomic DNA of 100 ng from hypothalamus or blood was used to determine total 5-methylcytosine (5-mC) using the 5-mC DNA ELISA kit (Zymo Research Corp., Irvine, CA, USA) as per the manufacturer's instruction.

### 2.9. Genome-wide DNA methylation profiling

A modified reduced representative bisulfite sequencing (RRBS) protocol (Methyl-MiniSeq) was used to prepare libraries from 200 to 500 ng of genomic DNA digested with 60 units of TaqαI and 30 units of MspI (NEB) sequentially and then extracted with the Zymo Research (ZR) DNA Clean & Concentrator-5 kit (Cat#: D4003). Fragments were ligated to preannealed adapters containing 5'-methyl-cytosine instead of cytosine according to Illumina's specified guidelines (www.illumina.com). Adapter-ligated fragments of 150–250 bp and 250–350 bp in size were recovered from a 2.5% NuSieve 1:1 agarose gel (Zymoclean Gel DNA Recovery Kit, ZR Cat#: D4001). The fragments were then bisulfite-treated using the EZ DNA Methylation-Lightning Kit (ZR, Cat#: D5020). Preparative-scale PCR was performed, and the resulting products were purified (DNA Clean & Concentrator; ZR, Cat#: D4005) for sequencing on an Illumina HiSeq.

### 2.10. RRBS sequence alignments and data analysis

Sequence reads from bisulfite-treated MiniSeq libraries were identified using the standard Illumina base-calling software and then analyzed using a Zymo Research proprietary analysis pipeline, which is written in Python and used Bismark (http://www.bioinformatics.babraham.ac.uk/projects/bismark/) to perform the alignment to the rn6 genome. Index files were constructed using the bismark_genome_preparation command and the entire reference genome. The –non_directional parameter was applied while running Bismark. All other parameters were set to default. Filled-in nucleotides were trimmed off when doing methylation calling. The methylation level of each sampled cytosine was estimated as the number of reads reporting a C, divided by the total number of reads

reporting a C or T. Fisher's exact test or *t*-test was performed for each CpG site, which has at least five reads coverage, and promoter, gene body, and CpG island annotations were added for each CpG included in the comparison.

## 3. Results

### 3.1. The perimenopause animal model

Cycle duration of 5-month-old female Sprague-Dawley rats was assessed longitudinally for 5 months. Based on cycle data, rats were stratified into groups according to the stage of ovarian senescence following the classification of the human perimenopause-menopause transition as per Stages of Reproductive Aging Workshop (STRAW) (Finch, 2014; Harlow et al., 2012). The endocrine aging groups included regular cyclers (4- to 5-day cycles), irregular cyclers (5- to 8-day cycles), and acyclic (no cycling within 9 days) at 9–10 months.

Cycling patterns were assessed daily, and stratification of endocrine status was analyzed at 6 months, 8 months, and 9 months of age. At 6 months, 82% of females were regular cyclers (Reg-6m) and the remaining 18% were irregular cyclers. At 8 months, 62% were regular cyclers, and the percentage of irregular cyclers increased to 43%, with the first appearance of acyclicity at 5%. At 9 months, the percent of regular cyclers declined to 37% (Reg-9m), the percent of irregular cyclers decreased to 30% (Irreg-9m), and the remaining 33% were acyclic (Acyc-9m) (Fig. 1A). An increase in body weight was observed between the 6- and 9-month-old regular cyclers ($p < 0.0001$) and was maintained across subsequent stages (Fig. 1D). There were no differences in body weight among 9-month-old animals at different endocrine stages ($p = 0.0515$). Uterine weight did not differ across the 5 endocrine phenotypes ($p = 0.30$) and was consistent with all animals being euthanized at estrus or constant estrus (Fig. 1B).

### 3.2. RNA-seq

A total of 20,877 transcripts in the hypothalamus were identified, sequenced, and analyzed (Fig. 2). Between 6 and 9 months, 2094 (10%) genes were significantly different ($p < 0.05$). Between 9 months' regular and irregular, and irregular and acyclic groups, 374 (2%) and 442 (2%) genes, respectively, were significantly different ($p < 0.05$) (Fig. 2). IPA was used to identify canonical signaling pathways associated with changes in gene expression between endocrine groups. 446 significant signaling pathways were identified within Reg-6m to Reg-9m, 256 within Reg-9m to Irreg-9m, and 195 within Irreg-9m to Acyc-9m group comparisons. Selected top canonical pathways, and the genes involved, are summarized in Supplemental Information (Supplemental Table 1).

The top upstream transcriptional regulator across all group comparisons was beta-estradiol (E2) (Table 1). E2 signaling was predicted to be involved in the downregulation of genes between 6 and 9 months, before perimenopause onset of irregular cycling. GnRH and KISS1 were also identified as regulators across all group comparisons. SAM and homocysteine were predicted to down-regulate related genes between the Reg-6m and Reg-9m groups, suggesting that impaired one-carbon metabolism may be responsible for transcriptional changes seen during this time frame, possibly through epigenetic mechanisms. S-adenosylhomocysteine, which is formed by the demethylation of SAM during methyl-group donation, was identified as a regulator during Reg-9m to Irreg-9m and Irreg-9m to Acyc-9m transitions.

### 3.3. Epigenetic changes across perimenopause

Hypothalamic samples underwent RRBS analysis (n = 5–6/group) with an average of 36 million (M) read pairs obtained for each sample (range = 31–46 M read pairs). The percentage of the raw reads, which were mapped to the rn6 genome ranged from 44% to 58%. An average of 4.7 million unique CpG sites were sequenced for each sample (range = 3.8–5.4 M) at an average depth of 13X (range = 10–16X).

Considering the regulatory role of CpG sites within the genome and the inbred genetic background of the animals used in this study, it was expected that the correlation (r) of CpG methylation patterns between two groups would approach 1 for the same tissue type. Despite this tight correlation, thousands of statistically significant differentially methylated CpG sites were still evident, indicative of epigenetic regulation of the transcriptional states in the different endocrine statuses. The regulatory role of non-CpG methylation is less clearly established, and CHG and CHH sites ("H" refers to different cytosine methylation contexts, namely CpG, CHG, and CHH), where H means "not G" (A, T, or C), are more prone to mutation. This was reflected in our data by a lower r-value for CHG and CHH comparisons between groups (Table 2), demonstrating that CHG and CHH patterns are less similar between groups. Heatmaps displaying hierarchical clustering of the top 100 significant CHG and CHH sites showed very little differences between groups, suggesting that the observed genome-wide differences occured largely on an individual basis and that only a few non-CpG sites play a role in endocrine status (Supplemental Figs. 1–3).

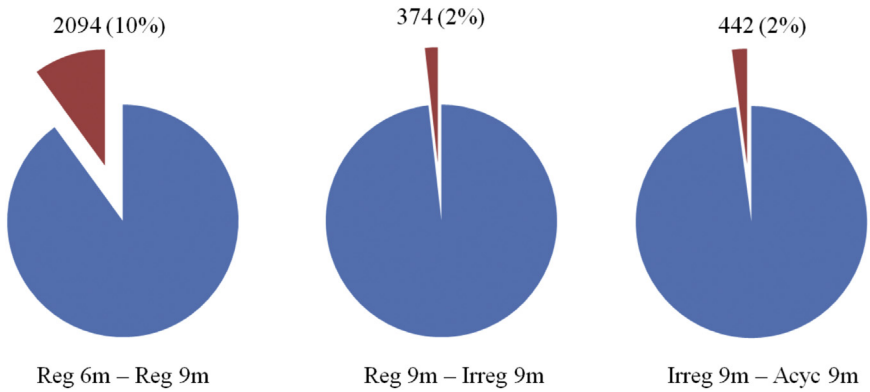


**Fig. 2.** Hypothalamic gene expression across endocrine aging cycling phenotypes. A total of 20,877 transcripts in the hypothalamus were identified and sequenced using Illumina HiSeq 2500 using 50 bp PE to obtain a total read depth of roughly 50 million read pairs per sample. Of the total number of transcripts sequenced, 2094 (10%), 374 (2%), and 442 (2%) genes were significantly different between the 6- and 9-month-old regular cyclic, 9-month-old regular and irregular cyclic, and 9-month-old irregular cyclic and acyclic groups, respectively ($p < 0.05$).

**Table 1**
Upstream regulators identified by Ingenuity Pathway Analysis (IPA)

| Symbol | Gene name | Reg-6m to Reg-9m | | Reg-9m to Irreg-9m | | Irreg-9m to Acyc-9m | |
|---|---|---|---|---|---|---|---|
| | | z-score | *p*-value | z-score | *p*-value | z-score | *p*-value |
| GnRH | Gonadotropin-releasing hormone 1 | −0.286 | 5.87E-05 | 1.647 | 4.36E-07 | −0.971 | 8.47E-05 |
| KISS1 | Kisspeptin | −1.969 | 0.153 | 1.969 | 0.000456 | −1.969 | 0.000779 |
| SAH | S-adenosylhomocysteine | | | | 0.0334 | | 0.0385 |
| SAM | S-adenosylmethionine | −1.287 | 0.0336 | | | | 0.0258 |
| Hcy | Homocysteine | −0.043 | 0.0206 | | | | |
| PRL | Prolactin | 3.936 | 8.25E-15 | | | | |
| E2 | 17β-estradiol | −2.08 | 8.65E-25 | 0.569 | 4.7E-18 | −0.042 | 1.05E-19 |

Activation z-score infers the activation states of predicted transcriptional regulators. Dependent on the observed expression of a gene in the data set, the activation state of a regulator is determined by the direction associated with the relationship to the regulator. Positive and negative z-scores indicate predicted activation or inhibition, respectively. Z-scores are not available for when no directional prediction can be made.

### 3.4. GnRH signaling and the HPG axis

In the hypothalamus, GnRH transcripts showed a dynamic pattern of expression. GnRH mRNA decreased by 1.7-fold between 6 and 9 months, increased by 1.9-fold at the onset of irregular cycling (Irreg-9m), and finally decreased once again by 1.5-fold in the acyclic animals (Acyc-9) (Table 3). Hypothalamic expression of the follicle-stimulating hormone subunit B (FSHB) was unchanged between 6 and 9 months but subsequently increased at the onset of irregular cycling followed by a decline in the acyclic group) (Table 3). No significant methylation differences in the GnRH1 or FSHB genes were observed (Table 3).

### 3.5. Increase in prolactin production

The hormone prolactin plays a key role in fertility by negatively regulating FSH and GnRH. Although primarily produced in the pituitary, the hypothalamus can produce significant amounts of prolactin (DeVito, 1988). In the pituitary, activation of dopamine receptor D2 (DRD2) suppresses prolactin gene expression and secretion (Fitzgerald and Dinan, 2008). Furthermore, thyrotropin-releasing hormone (TRH) produced in the hypothalamus acts on the pituitary to increase prolactin expression and secretion (Fitzgerald and Dinan, 2008).

Before perimenopause, between 6 and 9 months, there was a substantial 73.5-fold increase in hypothalamic prolactin expression. Accompanying this increase, factors that suppress prolactin secretion exhibited a modest −1.6-fold decrease in transcripts coding for both the prolactin-releasing hormone receptor (PRLHR) and a −1.4-fold prolactin receptor (PRLR) (Table 3). TRH declined −1.4-fold, and dopamine receptors D2 and D5 declined −1.3- and −1.4-fold, respectively (Table 3). During the transition from regular to irregular cycling, prolactin decreased but remained elevated compared with 6 month animals. Prolactin mRNA levels remained unchanged through the transition from irregular to acycling but remained elevated compared with pre-perimenopause levels. PRLHR, PRLR, DRD2, and DRD5 did not show any further changes in expression.

**Table 2**
Correlation of cytosine methylation (r-value)—CpG, CHG, and CHH correlations between endocrine groups

| Cytosine context | Reg-6m to Reg-9m | Reg-9m to Irreg-9m | Irreg-9m to Acyc-9m |
|---|---|---|---|
| | r-value | | |
| CpG | 0.9531 | 0.9521 | 0.9558 |
| CHG | 0.4441 | 0.4552 | 0.4978 |
| CHH | 0.4711 | 0.4760 | 0.5240 |

For replicates, one would expect r = 1, demonstrating perfect 1:1 correlation. Considering regulatory role of CpGs and the inbred genetic background of the animals, it is expected that CpG methylation between two groups be close to r = 1. CHG and CHH correlations have a lower r-value between groups.

TRH increased 1.2-fold from regular to irregular cycling and showed no significant changes during the irregular to acycling transition (Table 3).

There were no observed DNA methylation alterations in PRL or its' receptors PRLHR and PRLR that correlated to changes in expression levels. However, hypomethylation of DRD5 was observed during 6–9 months when DRD5 expression declined (Table 3).

### 3.6. Other hormones and receptors

Estrogen receptor β (Esr2) gene expression decreased −1.5-fold from 6 to 9 months and remained unchanged through perimenopause. Oxytocin (OXT) mRNA expression temporarily dropped during 6–9 months before recovering between Reg-9 and Irreg-9. Corticotropin-releasing hormone (CRH) and corticotropin-releasing hormone-binding protein (CRHBP) expression decreased −1.9- and −1.3-fold, respectively. A single site within the CRH promoter region was hypomethylated, and a single site within a CRHBP intron was hypermethylated between 6 and 9 months. No further changes in DNA methylation occurred in the two genes. CRH expression increased slightly (1.4-fold) between RC9 and IR9. Estrogen-related receptor gamma (ESRRG) transcriptionally activates DNA cytosine-5-methyltransferases 1 (Dnmt1) via binding to estrogen response elements in the DNMT1 promoters. Between 6 and 9 months, ESRRG transcription drops −1.3-fold and remains unchanged through the perimenopause transition. This decreased expression was accompanied by changes in 15 DNA methylation sites throughout the gene. Although ESRRG RNA levels remained unchanged through the transition, DNA methylation continued to change throughout perimenopause (Table 3).

### 3.7. Changes in glutamate signaling

From the RNA expression data, we inferred a substantial decrease in glutamate receptor signaling between 6 and 9 months, which did not recover during or post-perimenopause. Fifteen glutamate receptors and four glutamate transporter genes were significantly downregulated in the Reg-9m group compared with the Reg-6m group. Of these, three receptors and two solute carriers also underwent changes in DNA methylation between 6 and 9 months. Only one of the fifteen receptors (GRIND2) showed rebound increase at the onset of irregularity before decreasing again at the acyclic stage. Glutamate decarboxylase, GAD2, increased in irregular cycling animals. Two additional glutamate receptors, including GRIND2, continued to drop at acyclicity. An additional glutamate receptor (GRIK3) had unchanged expression until the onset of acyclicity, at which it declined. Several genes saw changes in DNA methylation across perimenopause that was not associated with changes in gene transcription (Table 4).

**Table 3**
Correlation between changes in DNA methylation and RNA expression in genes related to the HPG-axis and hormone signaling

| Gene symbol | Reg-6m to Reg-9m | | | | Reg-9m to Irreg-9m | | | | Irreg-9m to Acyc-9m | | | |
|---|---|---|---|---|---|---|---|---|---|---|---|---|
| | RNA | | DM | | RNA | | DM | | RNA | | DM | |
| GNRH1 | −1.7 | (0.0368) | - | | 1.9 | (0.0114) | - | | −1.6 | (0.0469) | - | |
| FSHB | | - | - | | 1.8 | (0.0124) | - | | −1.8 | (0.0157) | - | |
| PRL | 73.5 | (0.0106) | - | | −3.3 | (0.00085) | - | | | - | - | |
| PRLHR | −1.6 | (0.00655) | - | | | - | - | | | - | - | |
| PRLR | −1.4 | (0.0223) | - | | | - | (1) Intron | HYPER | | - | - | |
| TRH | −1.4 | (0.00005) | - | | 1.3 | (0.00005) | - | | −1.2 | (0.0007) | - | |
| TSHR | 1.6 | (0.00005) | - | | | - | (1) Intron | HYPER | | - | - | |
| DRD5 | −1.4 | (0.0464) | (1) Exon | HYPO | | - | - | | | - | - | |
| DRD2 | −1.3 | (0.0011) | - | | | - | - | | | - | - | |
| ESR2 | −1.5 | (0.0138) | - | | | - | - | | | - | - | |
| ESRRG | −1.3 | (0.00035) | (15) Intron | (8) HYPO<br>(7) HYPER | | - | (6) Intron | (5) HYPO<br>(1) HYPER | | - | (4) Intron | (1) HYPO<br>(3) HYPER |
| OXT | −3.5 | (0.00005) | - | | 3.5 | (0.00005) | - | | | - | - | |
| CRH | −1.9 | (0.00005) | (1) Promoter | HYPO | 1.4 | (0.00845) | - | | | - | - | |
| CRHBP | −1.3 | (0.0216) | (1) Intron | HYPER | | - | - | | | - | - | |
| KISS1 | 1.4 | (0.00805) | - | | | - | | - | | - | | - |

Fold changes and their respective *p*-values (RNA column) are listed for each endocrine group comparison. DNA methylation (DM) column at what endocrine status differential cytosine methylation was observed, within what region (promoter, exon, or intron), and whether the site(s) was hypomethylated or hypermethylated. Hypermethylated or hypomethylated is defined as 0%–33% more, or less, respectively, methylated than reference ($p$-value $< 0.05$).

### 3.8. Changes in GABA signaling

The RNA levels of four GABA receptors (GABRA1, GABRB2, GABRG2, and GABRG3) and one transporter gene (SLC32A1) were significantly downregulated between 6 and 9 months. SLC32A1 expression increased at the irregular cycling stage and decreased at the onset of acyclicity. In contrast, three GABA receptors (DBI, GABRA5, and GABRD) were upregulated between 6 and 9 months. GABRA5 expression decreased at irregular cycling and did not change further. A single site was hypermethylated and associated with decreased expression at 6–9 months in GABRG3. The remaining receptors and transporters exhibited no changes in DNA methylation across the perimenopause transition (Table 5).

### 3.9. Melatonin and circadian rhythm signaling

Postmenopausal women exhibit a loss of circadian rhythm control (Gomez-Santos et al., 2016) and are more likely to exhibit

**Table 4**
Correlation between changes in DNA methylation and RNA expression in genes related to glutamate signaling

| Gene symbol | Reg-6m to Reg-9m | | | | Reg-9m to Irreg-9m | | | | Irreg-9m to Acyc-9m | | | |
|---|---|---|---|---|---|---|---|---|---|---|---|---|
| | RNA | | DM | | RNA | | DM | | RNA | | DM | |
| GRIA1 | −1.2 | (0.0035) | - | | - | | (2) Intron | S HYPER | - | | - | |
| GRIA3 | −1.1 | (0.0430) | - | | - | | - | | - | | - | |
| GRIA4 | −1.3 | (0.0001) | - | | - | | - | | - | | (1) Promoter | HYPER |
| Grid1 | −1.1 | (0.0331) | - | | - | | (6) Intron | (5) HYPO<br>(1) HYPER | - | | (6) Intron | (3) HYPO<br>(3) HYPER |
| GRID2 | −1.2 | (0.0323) | (2) Intron | HYPER | - | | (4) Intron | (3) HYPO<br>(1) HYPER | - | | (2) Intron | (1) HYPO<br>(1) HYPER |
| GRID2IP | −1.6 | (0.0002) | - | | - | | (1) Exon | HYPO | - | | | |
| GRIK1 | −1.2 | (0.0071) | (1) Intron<br>(1) Exon | HYPER | - | | (1) Intron | HYPER | - | | (1) Intron | HYPO |
| GRIK3 | - | | (4) Intron | (2) HYPO<br>(2) HYPER | - | | (4) Intron | HYPER | −1.2 | (0.0432) | (2) Intron | HYPO |
| GRIN2A | −1.7 | (0.0001) | - | | - | | (1) Intron | HYPO | −1.3 | (0.0361) | (2) Intron | (1) HYPO<br>(1) HYPER |
| GRIN2B | −1.2 | (0.0035) | (6) Intron | (4) HYPO<br>(1) HYPER<br>(1) S HYPER | - | | - | | - | | - | |
| GRIN2D | −1.2 | (0.0060) | - | | 1.1 | (0.0192) | - | | −1.2 | (0.0222) | - | |
| GRIN3A | −1.3 | (0.0007) | - | | - | | - | | - | | - | |
| GRM1 | −1.2 | (0.0003) | - | | - | | - | | - | | (1) Intron | HYPER |
| GRM3 | −1.2 | (0.0058) | - | | - | | - | | - | | (1) Intron | HYPO |
| GRM5 | −1.2 | (0.0086) | - | | - | | - | | - | | (1) Promoter | HYPER |
| GRM7 | −1.2 | (0.0082) | - | | - | | (3) Intron | (1) S HYPO<br>(2) HYPO | - | | (1) Intron | HYPO |
| VGLUT1 | −3 | (0.0095) | - | | - | | - | | - | | - | |
| VGLUT3 | −1.4 | (0.0236) | (1) Promoter | HYPO | - | | - | | - | | - | |
| GLT1 | −1.2 | (0.0006) | (2) Intron | (1) HYPO<br>(1) HYPER | - | | - | | - | | - | |
| NAT2 | −1.2 | (0.0011) | - | | - | | - | | - | | (1) Intron | HYPER |

Fold changes and their respective *p*-values (RNA column) are listed for each endocrine group comparison. DNA methylation (DM) column at what endocrine status differential cytosine methylation was observed, within what region (promoter, exon, or intron), and whether the site(s) was hypomethylated, strongly(S) hypomethylated, hypermethylated, or strongly hypermethylated. Hypermethylated or hypomethylated is defined as 0%–33% more, or less, respectively, methylated than reference ($p$-value $< 0.05$). Strongly hypermethylated or strongly hypomethylated is defined as 33%–100% more, or less, respectively, methylated than reference ($p$-value $< 0.05$).

**Table 5**
Correlation between changes in DNA methylation and RNA expression in genes related to GABA signaling

| Gene symbol | Reg-6m to Reg-9m | | | | Reg-9m to Irreg-9m | | | Irreg-9m to Acyc-9m | | | |
|---|---|---|---|---|---|---|---|---|---|---|---|
| | RNA | | DM | | RNA | | DM | RNA | | DM | |
| DBI | 1.2 | (0.00005) | - | | - | | - | - | | - | |
| GABRA1 | −1.3 | (0.00005) | - | | - | | - | - | | - | |
| GABRA5 | 1.2 | (0.00005) | - | | −1.1 | 0.0443 | - | - | | - | |
| GABRB2 | −1.2 | (0.0041) | - | | - | | - | - | | - | |
| GABRD | 1.1 | (0.008) | - | | - | | - | - | | - | |
| GABRG2 | −1.3 | (0.00005) | - | | - | | - | - | | - | |
| GABRG3 | −1.8 | (0.00015) | (1) Intron | HYPER | - | | - | - | | (1) Intron | HYPO |
| SLC32A1 | −1.4 | (0.00515) | - | | 1.2 | 0.00035 | - | −1.2 | 0.00145 | - | |

Fold changes and their respective *p*-values (RNA column) are listed for each endocrine group comparison. DNA methylation (DM) column at what endocrine status differential cytosine methylation was observed, within what region (promoter, exon, or intron), and whether the site(s) was hypomethylated or hypermethylated. Hypermethylated or hypomethylated is defined as 0%–33% more, or less, respectively, methylated than reference ($p$-value $< 0.05$).**$p < 0.01$.

sleep disturbances, such as insomnia or poor sleep quality, compared with premenopausal women (Jehan et al., 2015). Both RNA and DNA methylation pathway analyses identified melatonin signaling and circadian rhythm as systems undergoing change during the perimenopause transition. Alterations in these systems first appeared during early hypothalamic aging, between 6 and 9 months. A majority (36/44) of the genes showed decreased RNA levels while DNA methylation changes consisted of both hypomethylation and hypermethylation in primarily intron regions. Although transcriptional changes predominantly occurred before onset of irregular cycling, changes in the DNA methylation continued to accumulate throughout the transition (Table 6).

### 3.10. Epigenome maintenance and one-carbon metabolism

Multiple genes involved in epigenetic maintenance of DNA methylation and histone modifications changed in expression across the perimenopause transition (Table 7). In total, fifteen genes were identified, including two DNA methyltransferases (DNMT), two ten-eleven translocation methylcytosine dioxygenases (Tet), seven histone methyltransferases, two histone deacetylases, and one histone demethylase. The majority of the changes occurred between 6 and 9 months with eleven genes exhibiting changes in genes involved in DNA methylation (Table 7). One gene, a histone methyltransferase, changed at the onset of irregular cycling, whereas five genes were downregulated in the acyclic group. The temporal pattern for change in epigenetic gene expression suggests that epigenetic reorganization begins between 6 and 9 months, before the onset of perimenopause.

Nine genes that are involved in one-carbon metabolism and SAM production significantly changed across endocrine aging (Table 8). Eight of these genes changed between 6 and 9 months. None of the identified genes were found to change during the transition to irregular cycling, and only one gene was found to change at the onset of acyclicity. Again, the data indicate that systems involved in epigenetic maintenance and reorganization are altered before manifestation of irregular cyclicity that characterizes the perimenopause.

### 3.11. Changes in hypothalamic global DNA methylation

In the hypothalamus, global DNA methylation significantly declined ($p = 0.0035$) at the onset of perimenopause, which is marked by irregular cycling (Fig. 3A). Decreased DNA methylation levels were sustained throughout the transition into complete reproductive senescence/menopause ($p = 0.0051$) (Fig. 5A). Further analysis revealed that between 6-9 months, while animals were still regularly cycling, two distinct populations of global DNA methylation were apparent and statistically different ($p = 0.0026$) (Fig. 5B). One-third (33%) of the 6- to 9-month-old animals exhibited global DNA methylation levels compared with Reg-9m animals. In contrast, two-thirds (66%) of the 6- to 9-month-old animals exhibited global DNA methylation levels compared with irregular cycling animals ($p = 0.0028$) (Fig. 5B). These findings suggest that individual differences in epigenetic profile may contribute to individual differences in endocrine aging.

### 3.12. DNA methylation and menopause timing

#### 3.12.1. 5-Aza-2'-deoxycitidine treatment

To determine if DNA methylation directly influenced the onset and progression of perimenopause, 6-month-old animals were treated with 5-aza-2'-deoxycitidine (5-aza), a demethylating agent. Animals were then assessed for cyclicity and perimenopause timing. 5-aza hypomethylates DNA by effectively depleting DNMT's, preventing methylation of cytosines. If perimenopause is epigenetically regulated, then treatment with 5-aza should disrupt timing of onset and/or completion of the perimenopause transition. Because the RNA-seq and global DNA methylation analyses suggested that hypothalamic aging occurred between 6 and 9 months, before the onset of irregular cycling, treatment was initiated at 6 months. Regular cycling animals were injected with 5-aza or vehicle three times a week for 3 months. Because hypothalamic DNA methylation dramatically declined at the onset of perimenopause (Fig. 3), we hypothesized that 5-aza-induced hypomethylation would induce premature of onset and/or completion of the perimenopause transition.

To monitor the effectiveness of the 5-aza treatments, we assessed DNA methylation levels in peripheral blood to predict hypomethylation in the brain. To verify that animals were indeed responding to 5-aza treatments, we collected serial blood collections and measured DNA methylation levels for 3 weeks after initiation of treatment. During the 3 weeks, we observed a continuous decline in global DNA methylation that was not observed in saline-treated animals. In 5-aza-treated animals, blood DNA methylation levels were significantly lower ($p = 0.0120$) at week 3 than week 1 (Fig. 4).

At 9 months of age, a significantly higher proportion of 5-aza-treated animals had transitioned into constant estrus and were no longer cycling (acyc), as assessed by the Chi-square analysis ($p = 0.033$). In contrast, all the vehicle-treated animals continued to cycle (regularly or irregularly) (Fig. 5). Survival curve analyses, using the log-rank (Mantel-Cox) test followed by the Gehan-Breslow-Wilcoxon test, indicated a nonsignificant trend toward accelerated onset of perimenopause in the 5-aza-treated animals (Fig. 6A). More striking acceleration was evident in the earlier age of exiting irregular cycling/perimenopause and entering into acyclicity/menopause in the 5-aza treated animals

**Table 6**
Correlation between changes in DNA methylation and RNA expression in genes involved in melatonin signaling and circadian rhythm

| Gene symbol | Reg-6m to Reg-9m | | | | Reg-9m to Irreg-9m | | | | Irreg-9m to Acyc-9m | | | |
|---|---|---|---|---|---|---|---|---|---|---|---|---|
| | RNA | | DM | | RNA | | DM | | RNA | | DM | |
| ABAT | −1.1 | (0.0358) | (1) Intron | | - | | - | | - | | - | |
| ADCY1 | −1.7 | (0.00005) | (3) Intron | (1)HYPO (2) HYPER | - | | - | | - | | (1) Exon | HYPER |
| ADCY3 | −1.1 | (0.0276) | (1) Intron | HYPO | - | | - | | - | | (1) Intron | HYPER |
| ATF2 | −1.2 | (0.00675) | - | | - | | - | | - | | (1) Intron | HYPER |
| AVP | −1.4 | (0.00005) | (1) Promoter | S HYPER | 1.7 | (0.00005) | - | | - | | - | |
| BHLHE40 | 1.1 | (0.0142) | - | | −1.2 | (0.0183) | - | | - | | - | |
| CAMK2D | −1.1 | (0.028) | (1) Intron | S HYPER | - | | (1) Intron | S HYPER | - | | (2) Intron | S HYPO |
| CAMK4 | −1.3 | (0.0216) | (3) Intron | (2) HYPO (1) HYPER | - | | - | | - | | (1) Intron | HYPO |
| CACNA1C | −1.1 | (0.0234) | (2) Exon (2) Intron | (3)HYPO (1)HYPER | - | | (4) Exon (3) Intron | (3) HYPO (4) HYPER | - | | (2) Exon (2) Promoter | (1) HYPO (3) HYPER |
| CDH1 | 2.1 | (0.00005) | (1) Exon | HYPER | −1.7 | (0.00005) | (1) Intron | HYPO | - | | - | |
| CREB1 | −1.3 | (0.0491) | - | | - | | - | | - | | - | |
| CREB5 | - | | - | | 1.2 | (0.0365) | (5) Intron | (2) HYPO (3) HYPER | - | | (2) Intron | HYPER |
| ELMO1 | −1.2 | (0.0142) | - | | - | | (2) Intron | (1) HYPO (1) HYPER | - | | (2) Intron | (1) HYPO (1) HYPER |
| EZR | 1.3 | (0.00005) | (2) Intron | HYPO | - | | (1) Exon (4) Intron | (3) HYPO (2) HYPER | - | | (2) Exon (3) Intron | (4) HYPO (1) HYPER |
| GNAI1 | −1.1 | (0.0189) | - | | - | | - | | - | | - | |
| GNAQ | −1.2 | (0.00425) | (1) Intron | HYPO | - | | - | | - | | (1) Intron | HYPO |
| GRIA1 | −1.2 | (0.0035) | (1) Intron | HYPO | - | | (2) Intron | (1) S HYPER (1) HYPER | - | | - | |
| GRIA3 | −1.1 | (0.043) | - | | - | | - | | - | | - | |
| GRIN2A | −1.7 | (0.00005) | - | | - | | (1) Intron | HYPO | −1.3 | (0.0361) | (2) Intron | (1) HYPO (1) HYPER |
| GRIN2B | −1.2 | (0.0035) | (6) Intron | (1) S HYPO (4) HYPO (1) HYPER | - | | - | | - | | - | |
| GRIN2D | −1.2 | (0.00595) | - | | 1.2 | (0.0192) | - | | −1.2 | (0.0222) | - | |
| GRIN3A | −1.3 | (0.00065) | - | | - | | - | | - | | - | |
| IGF1R | −1.2 | (0.00685) | - | | - | | (2) Intron | (1) HYPO (1) HYPER | - | | (1) Exon (8) Intron | (4) HYPO (5) HYPER |
| ITPR3 | 1.3 | (0.00655) | (2) Intron | (1) HYPO (1) HYPER | - | | (4) Intron | (3) HYPO (1) HYPER | - | | (1) Intron | HYPO |
| MAPK3 | 1.1 | (0.0417) | - | | - | | - | | - | | - | |
| NOS1 | −1.2 | (0.0172) | (2) Intron | HYPO | - | | (2) Intron | (1) HYPO (1) HYPER | - | | (1) Intron | HYPER |
| PCLO | −1.2 | (0.0002) | - | | 1.1 | (0.0137) | (1) Intron | HYPER | - | | (1) Exon | HYPO |
| PER3 | 1.1 | (0.014) | (1) Exon (1) Intron | (1) HYPO (1) HYPER | - | | (1) Exon (1) Intron | HYPO | - | | - | |
| PLCB1 | −1.2 | (0.00215) | (2) Intron | (1) HYPO (1) HYPER | - | | (2) Intron | HYPO | - | | (2) Intron | (1) HYPO (1) HYPER |
| PLCB3 | 1.2 | (0.004) | - | | - | | - | | - | | - | |
| PLCB4 | −1.1 | (0.0376) | (3) Intron | (2) HYPO (1) HYPER | - | | (3) Intron | (1) HYPO (2) HYPER | - | | (2) Intron | HYPO |
| PLCD1 | 1.2 | (0.0253) | - | | - | | - | | - | | - | |
| PLCL2 | −1.1 | (0.0282) | - | | - | | - | | - | | (1) Intron | HYPO |
| PPP2R2C | −1.2 | (0.0004) | (1) Intron | HYPO | - | | - | | - | | - | |
| PRKACB | −1.3 | (0.00005) | (1) Promoter (1) Intron | (1) HYPO (1) HYPER | - | | - | | - | | - | |
| PRKAR1B | −1.2 | (0.00485) | - | | - | | - | | - | | (2) Intron | HYPER |
| PRKAR2A | −1.2 | (0.00245) | - | | - | | - | | - | | - | |
| PRKCB | −1.3 | (0.00005) | (4) Intron | (1) HYPO (3) HYPER | - | | - | | - | | (1) Intron | HYPER |
| PRKCD | −1.6 | (0.00005) | - | | - | | - | | - | | - | |
| PRKCE | −1.2 | (0.0104) | (6) Intron | (5) HYPO (1) HYPER | - | | (8) Intron | (4) HYPO (4) HYPER | - | | (5) Intron | (2) HYPO (1) S HYPER (2) HYPER |
| PRKCH | −1.3 | (0.04) | (5) Intron | (1) HYPO (4) HYPER | - | | (3) Intron | (1) HYPO (2) HYPER | - | | (4) Intron | HYPO |
| PRKG2 | −1.2 | (0.025) | - | | - | | - | | - | | - | |
| SHC3 | −1.3 | (0.0019) | (2) Intron | HYPER | - | | - | | - | | (1) Intron | HYPO |
| VIP | −1.4 | (0.00005) | - | | - | | - | | 1.4 | (0.0024) | - | |

Fold changes and their respective *p*-values (RNA column) are listed for each endocrine group comparison. DNA methylation (DM) column denotes at what endocrine status differential cytosine methylation was observed, how many sites within what regions (promoter, exon, or intron), and whether the site(s) was hypomethylated, strongly(S) hypomethylated, hypermethylated, or strongly hypermethylated. Hypermethylated or hypomethylated is defined as 0%–33% more, or less, respectively, methylated than reference ($p$-value $< 0.05$). Strongly hypermethylated or strongly hypomethylated is defined as 33%–100% more, or less, respectively, methylated than reference ($p$-value $< 0.05$).

**Table 7**
Correlation between changes in DNA methylation and RNA expression in genes in epigenome regulation

| Gene symbol | Reg-6m to Reg-9m | | | | Reg-9m to Irreg-9m | | | | Irreg-9m to Acyc-9m | | | |
|---|---|---|---|---|---|---|---|---|---|---|---|---|
| | RNA | | DM | | RNA | | DM | | RNA | | DM | |
| DNMT3A | - | | - | | - | | - | | −1.1 | (0.0392) | - | |
| DNMT3B | - | | - | | - | | - | | −1.5 | (0.0212) | - | |
| TET1 | −1.4 | (0.00565) | - | | −1.1 | (0.0443) | - | | - | | - | |
| TET3 | - | | - | | - | | - | | −1.2 | (0.0232) | - | |
| MECP2 | −1.2 | (0.0106) | - | | - | | - | | - | | - | |
| EHMT1 | −1.2 | (0.0262) | - | | - | | - | | - | | | |
| PRMT8 | −1.2 | (0.041) | (1) Intron | HYPER | - | | (1) Intron | HYPO | - | | (1) Intron | HYPO |
| METTL7A | 1.2 | (0.00185) | - | | 1.2 | (0.00035) | - | | - | | | |
| METTL8 | −1.3 | (0.0311) | - | | - | | - | | - | | | |
| HDAC1 | 1.2 | (0.0089) | - | | - | | - | | - | | | |
| HDAC5 | −1.2 | (0.00025) | (1) Intron | HYPO | - | | (1) Intron | HYPER | - | | | |
| KDM6B | 1.1 | (0.0137) | - | | - | | - | | - | | | |
| KMT2A | −1.1 | (0.0126) | - | | 1.15 | (0.00615) | - | | −1.16 | (0.0079) | | |
| KMT2B | - | | - | | - | | - | | −1.12 | (0.038) | | |

Fold changes and their respective *p*-values (RNA column) are listed for each endocrine group comparison. DNA methylation (DM) column at what endocrine status differential cytosine methylation was observed, within what region (promoter, exon, or intron), and whether the site(s) was hypomethylated or hypermethylated. Hypermethylated or hypomethylated is defined as 0%–33% more, or less, respectively, methylated than reference ($p$-value $< 0.05$).

(Mantel-Cox $p = 0.0043$; Gehan-Breslow-Wilcoxon $p = 0.006$) (Fig. 6B). These results indicate that perimenopause duration and menopause timing are regulated by epigenetic mechanisms including DNA methylation.

#### 3.12.2. Methionine treatment

RNA-seq and genome-wide DNA methylation analyses suggested that impaired one-carbon metabolism could be involved in the onset of perimenopause. Impaired one-carbon metabolism, resulting in a decrease of SAM production, may be responsible for the loss of DNA methylation observed in perimenopausal animals. To test whether perimenopause onset and/or completion could be delayed, animals were treated with methionine (a precursor of SAM), in an attempt to supplement the aging epigenome and prevent DNA hypomethylation. Treatment was initiated at 6 months and continued until 10 months at which time cyclicity was assessed. At 10 months, a significantly larger proportion of methionine-treated animals (86%) were still regularly cycling compared with the control group (25%), as assessed by the Chi-square test ($p = 0.044$). There were no irregularly cyclers, and all remaining animals were acyclic (Fig. 7).

## 4. Discussion

### 4.1. Hypothalamic endocrine aging begins before perimenopause

Reproductive senescence is a function of both hypothalamic and ovarian aging and is influenced by environmental, genetic, and lifestyle factors, as well as systemic diseases. The majority of changes in hypothalamic gene expression occurred during the 6- to 9-month period when animals were still cycling regularly, indicating that hypothalamic aging begins before the phenotypic manifestation of perimenopause. Furthermore, regulators involved in HPG-axis signaling, GnRH, E2, and KISS1 were identified as upstream regulators during this time suggesting that altered HPG signaling precedes ovarian aging.

Prolactin expression is remarkably upregulated before irregular cycling, making it a promising candidate as a perimenopause initiator. Hyperprolactinemia is a known reproductive inhibitor in both males and females and is responsible for loss of libido as well as infertility in humans (Anderson et al., 2008). Although prolactin signaling is not well described within the hypothalamus, we propose that hypothalamic hyperprolactinemia plays a similar role in reproductive senescence, by negatively regulating GnRH and FSH. We saw no changes in the DNA methylation patterns in the genes coding for prolactin or prolactin's receptors indicating that the observed changes were regulated by other factors, such as histone modifications or transcription factor binding. In the pituitary, prolactin secretion and gene expression are regulated by multiple factors including dopamine and TRH and their receptors (Fitzgerald and Dinan, 2008; Yu et al., 2010). Consistent with what is known for pituitary prolactin, data reported herein indicate that both TRH and dopamine receptor D5 (DRD5) expressions change across the transition.

However, multiple genes coding for histone-modifying proteins during this period were modified. Candidate epigenetic regulator

**Table 8**
Correlation between changes in DNA methylation and RNA expression in genes related to one-carbon metabolism

| Gene symbol | Reg-6m to Reg-9m | | | Reg-9m to Irreg-9m | | | Irreg-9m to Acyc-9m | | | |
|---|---|---|---|---|---|---|---|---|---|---|
| | RNA | | DM | RNA | DM | | RNA | | DM | |
| MTHFR | - | | - | - | - | | −1.2 | (0.0481) | - | |
| SLC44A2 | 1.1 | (0.0314) | - | - | (1) Intron | HYPO | - | | (1) Intron | HYPER |
| FOLR2 | 2.5 | (0.003) | - | - | (1) Intron | HYPO | - | | (1) Intron | HYPER |
| TYMS | −1.4 | (0.0067) | - | - | - | | - | | - | |
| MUT | −1.1 | (0.0462) | - | - | - | | - | | - | |
| PLD1 | 1.2 | (0.0144) | - | - | (2) Intron | HYPO | - | | (2) Intron | HYPER |
| PLD2 | 1.2 | (0.00605) | - | - | - | | - | | (1) Exon (1) Intron | (1) HYPO (1) HYPER |
| PLD4 | 1.2 | (0.0273) | - | - | - | | - | | - | |
| NAPEPLD | −1.3 | (0.0252) | - | - | - | | - | | - | |

Fold changes and their respective *p*-values (RNA column) are listed for each endocrine group comparison. DNA methylation (DM) column at what endocrine status differential cytosine methylation was observed, within what region (promoter, exon, or intron), and whether the site(s) was hypomethylated or hypermethylated. Hypermethylated or hypomethylated is defined as 0%–33% more, or less, respectively, methylated than reference ($p$-value $< 0.05$).

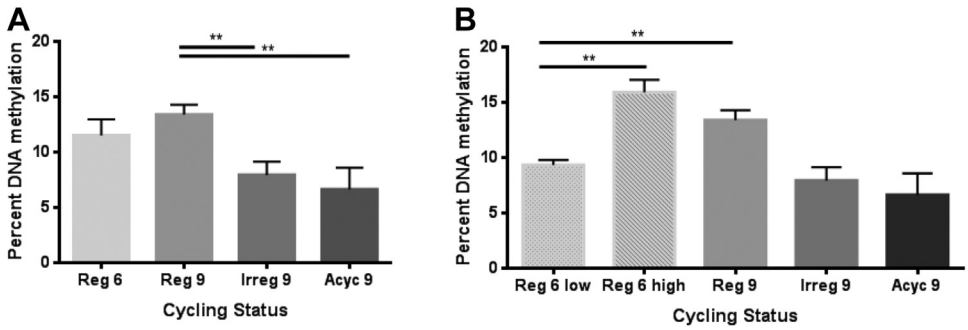


**Fig. 3.** Magnitude of global DNA methylation across endocrine aging cycling phenotypes. (A) Hypothalamic DNA methylation declined at the onset of perimenopause ($p = 0.0035$) and remains low through completion of the transition ($p = 0.0051$). (B) Two statistically different populations exist within the 6-month regular group ($p = 0.0026$). When compared separately, the 6-month regular "low" population has statistically decreased levels of global DNA methylation ($p = 0.0028$).$^{**}p < 0.01$.

genes that could play role in prolactin's increased expression included one demethylase (KDM6B), five methyltransferases (EHMT1, PRMT8, METTL7A, METTL8, and KMT2A), two deacetylases (HDAC1 and HDAC5), and the methyl-binding domain protein (MECP2).

### 4.2. Hypothalamic neurological aging begins before irregular cycling

In the hypothalamus, a number of gene pathways exhibited changes prior to onset of irregular cycling, including those related to one-carbon metabolism, epigenetic regulation, as well as glutamatergic and GABAergic signaling. Numerous glutamate transporters and receptors were downregulated prior to irregular cycling and GABA receptors exhibited changes in both increased and decreased expression. Glutamate transporters are responsible for removing glutamate from the extracellular/synaptic space to prevent chronic activation of postsynaptic glutamate receptors and excitotoxicity. Particularly critical to glutamate reuptake is the transporter GLT1, which has been reported to constitute 1% of total brain protein (Sheldon and Robinson, 2007). We observed a significant decrease in four glutamate transporter genes, including GLT1, between 6 and 9 months (Table 4). Expression changes were accompanied by differential DNA methylation in two of the transporters, VGLUT3 and GLT1. We hypothesize that these changes in glutamate and GABA signaling before perimenopause sensitize the brain to environmental or hormonal insult, modifying the risk and/or rate of neurological decline as glutamate-mediated excitotoxicity has been linked to several neurodegenerative disorders such as Alzheimer's, amyotrophic lateral sclerosis, multiple sclerosis, and Parkinson's (Hynd et al., 2004; Lau and Tymianski, 2010) and impaired GABAergic signaling is reported to be a key feature of all neurodegenerative etiologies (Blaszczyk, 2016).

### 4.3. Accelerated epigenomic aging in early transitioners

Global DNA methylation declines with age (Pogribny et al., 2011; Wilson and Jones, 1983). In the hypothalamus, we do not observe a significant change in DNA methylation between 6-month regular and 9-month regularly cycling animals (Fig. 3A). However, within the Reg-6m animals, we see two distinct populations—with "high" and "low" global DNA methylation levels that are significantly different from each other. Individual animals appear to be aging at various rates and a subset of the 6-month animals' epigenomes appears to be biologically and endocrinologically "older". Indeed, at 6 months, two-thirds of the animals showed lower DNA methylation levels that were equivalent to Irreg-9m and Acyc-9m groups. The remaining one-third Reg-6m animals had DNA methylation levels similar to Reg-9m animals (Fig. 2B). Furthermore, this ratio of 1:3/2:3 matches the percentage of Reg-9m animals (37) versus Irreg-9m (30%) or Acyc-9m animals (33%) (Fig. 1A), suggesting that if left undisturbed, animals with lower global DNA methylation levels at 6 months would transition to irregular or acyclic sooner than those with higher levels. Similarly, we would expect 6 month animals with higher levels of DNA methyltion to continue to be regularly cycling at 9 months of age. These data suggest that individual epigenetic differences that are present before perimenopause predispose an individual toward a particular perimenopause outcome (late vs. early).

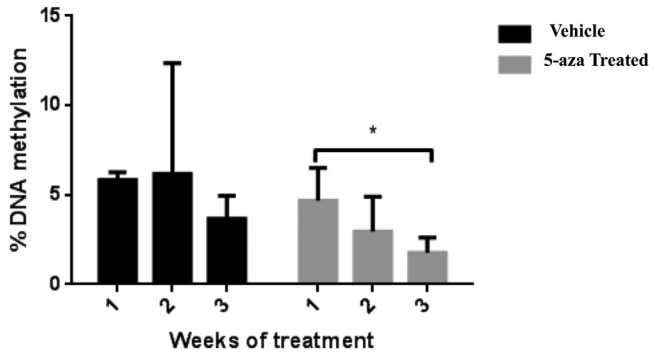


**Fig. 4.** Impact of 5-aza-2'-deoxycitidine (5-aza) on global DNA methylation in blood following systemic treatment. DNA methylation in peripheral blood was significantly hypomethylated by week 3 of 5-aza treatment ($p = 0.0120$; N = 6).$^{*}p < 0.05$.

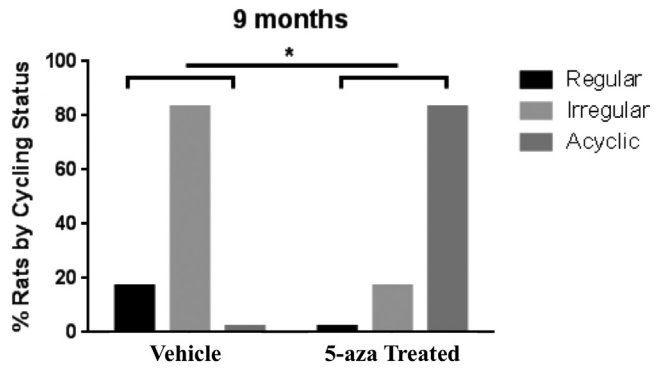


**Fig. 5.** Inhibition of DNA methylation and impact on endocrine aging phenotype. Using reduced representation bisulfite sequencing (RRBS), DNA methylation at cytosine residues was determined. At 9 months of age, the 5-aza-treated group had a significantly higher proportion of acyclic animals, whereas the vehicle-treated group had a significantly higher proportion of irregular cycling animals ($p = 0.033$; Chi-square test).$^{*}p < 0.05$.

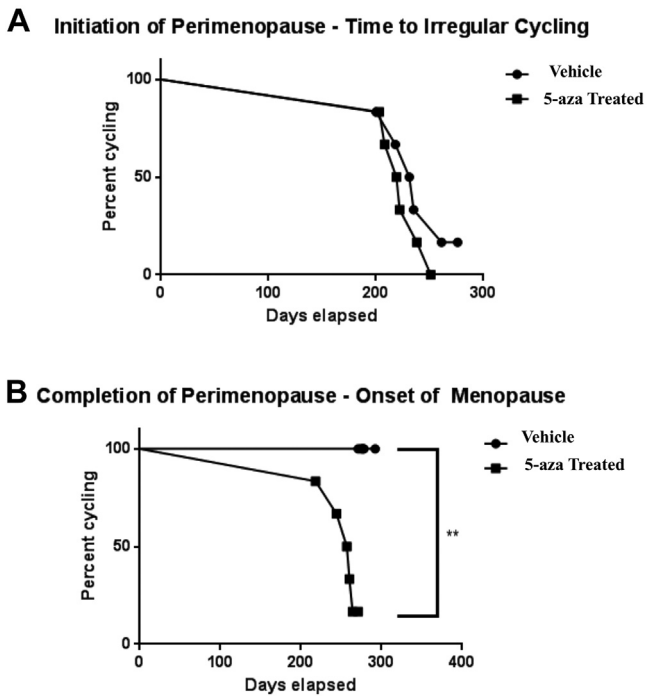


**Fig. 6.** Impact of 5-aza-2'-deoxycitidine (5-aza) on initiation and completion of perimenopause. (A) Survival curve analysis indicated a nonsignificant acceleration to initiation of perimenopause in 5-aza-treated animals. (B) 5-aza significantly accelerated progression through the perimenopausal transition to menopausal acyclicity (Mantel-Cox $p = 0.0043$; Gehan-Breslow-Wilcoxon $p = 0.006$).**$p < 0.01$.

In humans, menopause is associated with epigenetic patterns of aging in blood (Levine et al., 2016). Women with an earlier age of menopause onset were found to be "epigenetically older" than women with a later onset (Levine et al., 2016), despite being the same chronological age. Here, we show that, in rats, global DNA methylation declines at the onset of perimenopause, supporting the hypothesis that menopause and epigenetic age are inversely correlated. However, the cause-effect relationship of epigenetic and menopausal age remains ambiguous. To better understand this relationship, we sought to perturb the epigenome in our animals and assess if perimenopause timing was altered. We used 5-aza, which has been shown to shorten the lifespan of cells via hypomethylation of DNA (Fairweather et al., 1987), to induce an accelerated aging phenotype. In doing so, we were able to accelerate the perimenopause transition, bringing on an early "menopause" status in our animals (Fig. 5B).

Because an "older" epigenome is correlated with earlier menopause and associated with impaired one-carbon metabolism and loss of SAM, we also supplemented animals with methionine in an attempt to slow epigenetic aging and prolong reproductive competency. Methionine, a precursor to SAM, was chosen rather than SAM itself because it is much less volatile, has a greater half-life, and a lower dose is required to obtain systemic effects (Young and Shalchi, 2005). Reg-6m animals that were supplemented with methionine remained reproductively competent longer than their vehicle-treated counterparts (Fig. 6). Together, these data further clarify the cause-effect relationship of epigenetic and menopause age and provide evidence that epigenetic mechanisms regulate the perimenopause transition.

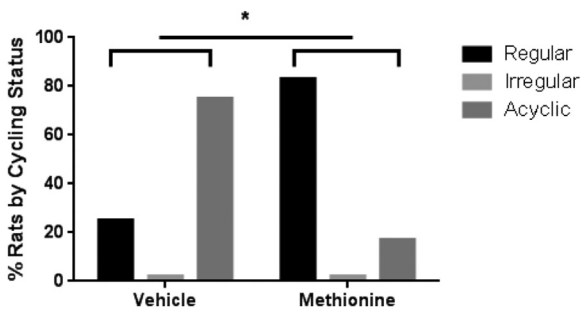


**Fig. 7.** Methionine treatment delayed onset of perimenopause. At 10 months, 86% of methionine-treated animals continued to cycle regularly compared with 25% of vehicle-treated animals ($p = 0.044$). Remaining animals were all acyclic.*p < 0.05.

### 4.4. Hypothalamic aging precedes hippocampal aging

The greatest changes in both gene expression and DNA methylation in the hypothalamus occurred prior to the onset of irregular cycling, the predominant phenotypic feature of perimenopause.

These early initiating events in the hypothalamus precede gene expression changes in the hippocampus, which are coincident with the onset of irregular cycling (Yin et al., 2015). In the hippocampus, we reported evidence of decline in bioenergetic systems and synaptic plasticity in the hippocampus during the transition from regular to irregular cycling (Yin et al., 2015). In addition, during the perimenopausal transition, we observed decline in brain glucose uptake and deficits in mitochondrial function. Further dynamic changes in genes and pathways related to glucose metabolism, fatty acid metabolism, inflammation, and mitochondrial function occurred across the perimenopausal to menopausal to postmenopausal transitions (Yin et al., 2015). Unlike the hypothalamus, the critical period of change in the hippocampus begins at the initiation of irregular cycling. It is likely that hippocampal aging is driven by the hormonal changes that occur as a result of reproductive senescence initiated by hypothalamic changes that occur before irregular cycling.

### 4.5. DNA methylation controls specific aspects of endocrine aging and reproductive senescence

Treatment with either 5-aza or methionine, known epigenetic modifiers, impacted the timing of reproductive senescence with inhibition of DNA methylation accelerating endocrine aging, whereas promoting DNA methylation with methionine delayed endocrine aging. Numerous studies have shown that peripheral 5-aza treatment, which crosses the blood-brain barrier, suppresses DNA methylation in all regions of the brain that have been studied (Fonteneau et al., 2017; Li et al., 2017; Lomniczi and Ojeda, 2016; Zhang et al., 2016).

The use of 5-aza, to induce hypomethylation as a model of accelerated aging, was a means to test our hypothesis that epigenetic changes regulate reproductive senescence. Because 5-aza globally hypomethylates DNA in a nonspecific manner, genome-wide methylation studies are likely to be inconclusive. For this reason, we focused on investigating patterns of genome-wide DNA methylation in animals undergoing biological endocrine aging to identify specific pathways directly related to natural reproductive senescence. Conversly, studies have shown that methionine can effectively reverse and prevent disease-associated epigenetic patterns in numerous models (Fuso et al., 2012; Gregoire et al., 2017; Parrish et al., 2015; Wright et al., 2015). We hypothesize that DNA methylation and RNA expression patterns in methionine treated animals to be comparable to naturally aging counterparts, as treatment delayed advancment to the next stage of reproductive senescence.

## 5. Conclusion

Collectively, the transcriptional and epigenetic changes reported herein indicate that the hypothalamus undergoes endocrine aging prior to onset of symptoms of reproductive senescence. Importantly, we show that this phenotypically silent period of genomic regulation represents a critical period in endocrine aging. Inhibition of DNA methylation accelerated transition through the perimenopause to complete reproductive senescence. In contrast, promoting DNA methylation through methionine supplementation delayed progression of endocrine aging and markedly sustained regular cycling, an endocrine phenotype of reproductive competence.

From a translational perspective, these data indicate that hypothalamic aging occurs prior to the onset of the perimenopausal phenotype of irregular cycling. Initiation of interventions to sustain epigenetic mechanisms, specifically DNA methylation, could be a strategy to sustain endocrine and neurological function in women (Fuso et al., 2008; Fuso et al., 2011; Fuso et al., 2012).

## Disclosure statement

The authors have no conflicts of interest to disclose.

## Acknowledgements

This study has been supported by NIA P01AG026572 to RDB: Project 1 to RDB and Analytic Core C to FY. The authors declare no competing financial interests and nothing to disclose.

## Appendix A. Supplementary data

Supplementary data to this article can be found online at doi.org/10.1016/j.neurobiolaging.2018.09.029.

## References

Anderson, G.M., Kieser, D.C., Steyn, F.J., Grattan, D.R., 2008. Hypothalamic prolactin receptor messenger ribonucleic acid levels, prolactin signaling, and hyperprolactinemic inhibition of pulsatile luteinizing hormone secretion are dependent on estradiol. Endocrinology 149, 1562–1570.

Blaszczyk, J.W., 2016. Parkinson's disease and neurodegeneration: GABA-Collapse hypothesis. Front Neurosci. 10, 269.

Bottner, M., Leonhardt, S., Wuttke, W., Jarry, H., 2007. Changes of expression of genes related to the activity of the gonadotrophin-releasing hormone pulse generator in young versus middle-aged male rats. J. Neuroendocrinol. 19, 779–787.

Brinton, R.D., Yao, J., Yin, F., Mack, W.J., Cadenas, E., 2015. Perimenopause as a neurological transition state. Nat. Rev. Endocrinol. 11, 393–405.

Byars, S.G., Ewbank, D., Govindaraju, D.R., Stearns, S.C., 2010. Colloquium papers: natural selection in a contemporary human population. Proc. Natl. Acad. Sci. U. S. A. 107 (Suppl 1), 1787–1792.

Davis, S.R., Lambrinoudaki, I., Lumsden, M., Mishra, G.D., Pal, L., Rees, M., Santoro, N., Simoncini, T., 2015. Menopause. Nat. Rev. Dis. Primers 1, 15004.

DeVito, W.J., 1988. Distribution of immunoreactive prolactin in the male and female rat brain: effects of hypophysectomy and intraventricular administration of colchicine. Neuroendocrinology 47, 284–289.

Fairweather, D.S., Fox, M., Margison, G.P., 1987. The in vitro lifespan of MRC-5 cells is shortened by 5-azacytidine-induced demethylation. Exp. Cell Res. 168, 153–159.

Finch, C.E., 2014. The menopause and aging, a comparative perspective. J. Steroid Biochem. Mol. Biol. 142, 132–141.

Fitzgerald, P., Dinan, T.G., 2008. Prolactin and dopamine: what is the connection? A review article. J. Psychopharmacol. 22 (2 Suppl), 12–19.

Fonteneau, M., Filliol, D., Anglard, P., Befort, K., Romieu, P., Zwiller, J., 2017. Inhibition of DNA methyltransferases regulates cocaine self-administration by rats: a genome-wide DNA methylation study. Genes Brain Behav. 16, 313–327.

Fuso, A., Nicolia, V., Cavallaro, R.A., Ricceri, L., D'Anselmi, F., Coluccia, P., Calamandrei, G., Scarpa, S., 2008. B-vitamin deprivation induces hyperhomocysteinemia and brain S-adenosylhomocysteine, depletes brain S-adenosylmethionine, and enhances PS1 and BACE expression and amyloid-beta deposition in mice. Mol. Cell Neurosci. 37, 731–746.

Fuso, A., Nicolia, V., Pasqualato, A., Fiorenza, M.T., Cavallaro, R.A., Scarpa, S., 2011. Changes in Presenilin 1 gene methylation pattern in diet-induced B vitamin deficiency. Neurobiol. Aging 32, 187–199.

Fuso, A., Nicolia, V., Ricceri, L., Cavallaro, R.A., Isopi, E., Mangia, F., Fiorenza, M.T., Scarpa, S., 2012. S-adenosylmethionine reduces the progress of the Alzheimer-like features induced by B-vitamin deficiency in mice. Neurobiol. Aging 33, 1482.e1–1482.e16.

Gaskins, A.J., Mumford, S.L., Chavarro, J.E., Zhang, C., Pollack, A.Z., Wactawski-Wende, J., Perkins, N.J., Schisterman, E.F., 2012. The impact of dietary folate intake on reproductive function in premenopausal women: a prospective cohort study. PLoS One 7, e46276.

Gomez-Santos, C., Saura, C.B., Lucas, J.A., Castell, P., Madrid, J.A., Garaulet, M., 2016. Menopause status is associated with circadian- and sleep-related alterations. Menopause 23, 682–690.

Gregoire, S., Millecamps, M., Naso, L., Do Carmo, S., Cuello, A.C., Szyf, M., Stone, L.S., 2017. Therapeutic benefits of the methyl donor S-adenosylmethionine on nerve injury-induced mechanical hypersensitivity and cognitive impairment in mice. Pain 158, 802–810.

Hak, A.E., Polderman, K.H., Westendorp, I.C., Jakobs, C., Hofman, A., Witteman, J.C., Stehouwer, C.D., 2000. Increased plasma homocysteine after menopause. Atherosclerosis 149, 163–168.

Harlow, S.D., Gass, M., Hall, J.E., Lobo, R., Maki, P., Rebar, R.W., Sherman, S., Sluss, P.M., de Villiers, T.J., Group, S.C., 2012. Executive summary of the Stages of Reproductive Aging Workshop + 10: addressing the unfinished agenda of staging reproductive aging. Menopause 19, 387–395.

Herrmann, W., Obeid, R., 2011. Homocysteine: a biomarker in neurodegenerative diseases. Clin. Chem. Lab Med. 49, 435–441.

Hynd, M.R., Scott, H.L., Dodd, P.R., 2004. Glutamate-mediated excitotoxicity and neurodegeneration in Alzheimer's disease. Neurochem. Int. 45, 583–595.

Jehan, S., Masters-Isarilov, A., Salifu, I., Zizi, F., Jean-Louis, G., Pandi-Perumal, S.R., Gupta, R., Brzezinski, A., McFarlane, S.I., 2015. Sleep disorders in Postmenopausal women. J. Sleep Disord. Ther. 4.

Lau, A., Tymianski, M., 2010. Glutamate receptors, neurotoxicity and neurodegeneration. Pflugers Arch. 460, 525–542.

Levine, M.E., Lu, A.T., Chen, B.H., Hernandez, D.G., Singleton, A.B., Ferrucci, L., Bandinelli, S., Salfati, E., Manson, J.E., Quach, A., Kusters, C.D., Kuh, D., Wong, A., Teschendorff, A.E., Widschwendter, M., Ritz, B.R., Absher, D., Assimes, T.L., Horvath, S., 2016. Menopause accelerates biological aging. Proc. Natl. Acad. Sci. U. S. A. 113, 9327–9332.

Li, Y., Ma, Q., Dasgupta, C., Halavi, S., Hartman, R.E., Xiao, D., Zhang, L., 2017. Inhibition of DNA methylation in the Developing rat brain disrupts Sexually Dimorphic Neurobehavioral phenotypes in Adulthood. Mol. Neurobiol. 54, 3988–3999.

Lomniczi, A., Ojeda, S.R., 2016. The Emerging role of epigenetics in the regulation of female puberty. Endocr. Dev. 29, 1–16.

Nazef, K., Khelil, M., Chelouti, H., Kacimi, G., Bendini, M., Tazir, M., Belarbi, S., El Hadi Cherifi, M., Djerdjouri, B., 2014. Hyperhomocysteinemia is a risk factor for Alzheimer's disease in an Algerian population. Arch. Med. Res. 45, 247–250.

Parrish, R.R., Buckingham, S.C., Mascia, K.L., Johnson, J.J., Matyjasik, M.M., Lockhart, R.M., Lubin, F.D., 2015. Methionine increases BDNF DNA methylation and improves memory in epilepsy. Ann. Clin. Transl. Neurol. 2, 401–416.

Pogribny, I.P., Muskhelishvili, L., Tryndyak, V.P., Beland, F.A., 2011. The role of epigenetic events in genotoxic hepatocarcinogenesis induced by 2-acetylaminofluorene. Mutat. Res. 722, 106–113.

Sheldon, A.L., Robinson, M.B., 2007. The role of glutamate transporters in neurodegenerative diseases and potential opportunities for intervention. Neurochem. Int. 51, 333–355.

Shen, L., Ji, H.F., 2015. Associations between homocysteine, folic acid, vitamin B12 and Alzheimer's disease: Insights from Meta-analyses. J. Alzheimers Dis. 46, 777–790.

Snieder, H., MacGregor, A.J., Spector, T.D., 1998. Genes control the cessation of a woman's reproductive life: a twin study of hysterectomy and age at menopause. J. Clin. Endocrinol. Metab. 83, 1875–1880.

Tomizawa, H., Matsuzawa, D., Ishii, D., Matsuda, S., Kawai, K., Mashimo, Y., Sutoh, C., Shimizu, E., 2015. Methyl-donor deficiency in adolescence affects memory and epigenetic status in the mouse hippocampus. Genes Brain Behav. 14, 301–309.

Wilson, V.L., Jones, P.A., 1983. DNA methylation decreases in aging but not in immortal cells. Science 220, 1055–1057.

Wright, K.N., Hollis, F., Duclot, F., Dossat, A.M., Strong, C.E., Francis, T.C., Mercer, R., Feng, J., Dietz, D.M., Lobo, M.K., Nestler, E.J., Kabbaj, M., 2015. Methyl supplementation attenuates cocaine-seeking behaviors and cocaine-induced c-Fos activation in a DNA methylation-dependent manner. J. Neurosci. 35, 8948–8958.

Yin, F., Yao, J., Sancheti, H., Feng, T., Melcangi, R.C., Morgan, T.E., Finch, C.E., Pike, C.J., Mack, W.J., Cadenas, E., Brinton, R.D., 2015. The perimenopausal aging transition in the female rat brain: decline in bioenergetic systems and synaptic plasticity. Neurobiol. Aging 36, 2282–2295.

Young, S.N., Shalchi, M., 2005. The effect of methionine and S-adenosylmethionine on S-adenosylmethionine levels in the rat brain. J. Psychiatry Neurosci. 30, 44–48.

Yu, X., Murao, K., Imachi, H., Li, J., Nishiuchi, T., Dobashi, H., Hosomi, N., Masugata, H., Zhang, G.X., Iwama, H., Ishida, T., 2010. The transcription factor prolactin regulatory element-binding protein mediates prolactin transcription induced by thyrotropin-releasing hormone in GH3 cells. Endocrine 38, 53–59.

Zeisel, S.H., 2009. Importance of methyl donors during reproduction. Am. J. Clin. Nutr. 89, 673S–677S.

Zhang, Z., Yang, J., Liu, X., Jia, X., Xu, S., Gong, K., Yan, S., Zhang, C., Shao, G., 2016. Effects of 5-Aza-2'-deoxycytidine on expression of PP1gamma in learning and memory. Biomed. Pharmacother. 84, 277–283.